# Molecular Basis for the Polymerization of Octopus Lens S-Crystallin

Hui-Chuan Chang,* Tai-Lang Lin,[†] and Gu-Gang Chang*
*Graduate Institutes of Life Sciences and Biochemistry, National Defense Medical Center, and [†]Institute of Zoology, Academia Sinica, Taipei, Taiwan, Republic of China

ABSTRACT   S-Crystallin from octopus lens has a tertiary structure similar to sigma-class glutathione transferase (GST). However, after isolation from the lenses, S-crystallin was found to aggregate more easily than sigma-GST. In vitro experiments showed that the lens S-crystallin can be polymerized and finally denatured at increasing concentration of urea or guanidinium chloride (GdmCl). In the intermediate concentrations of urea or GdmCl, the polymerized form of S-crystallin is aggregated, as manifested by the increase in light scattering and precipitation of the protein. There is a delay time for the initiation of polymerization. Both the delay time and rate of polymerization depend on the protein concentration. The native protein showed a maximum fluorescence emission spectrum at 341 nm. The GdmCl-denatured protein exhibited two fluorescence maxima at 310 nm and 358 nm, respectively, whereas the urea-denatured protein showed a fluorescence peak at 358 nm with a small peak at 310 nm. The fluorescence intensity was quenched. Monomers, dimers, trimers, and polymers of the native protein were observed by negative-stain electron microscopic analysis. The aggregated form, however, showed irregular structure. The aggregate was solubilized in high concentrations of urea or GdmCl. The redissolved denatured protein showed an identical fluorescence spectrum to the protein solution that was directly denatured with high concentrations of urea or GdmCl. The denatured protein was readily refolded to its native state by diluting with buffer solution. The fluorescence spectrum of the renatured protein solution was similar to that of the native form. The phase diagrams for the S-crystallin in urea and GdmCl were constructed. Both salt concentration and pH value of the solution affect the polymerization rate, suggesting the participation of ionic interactions in the polymerization. Comparison of the molecular models of the S-crystallin and sigma-GST suggests that an extra ion-pair between Asp-101 and Arg-14 in S-crystallin contributes to stabilizing the protomer. Furthermore, the molecular surface of S-crystallin has a protruding Lys-208 on one side and a complementary patch of aspartate residues (Asp-90, Asp-94, Asp-101, Asp-102, Asp-179, and Asp-180) on the other side. We propose a molecular model for the S-crystallin polymer in vivo, which involves side-by-side associations of Lys-208 from one protomer and the aspartate patch from another protomer that allows the formation of a polymeric structure spontaneously into a liquid crystal structure in the lens.

## INTRODUCTION

Crystallins are soluble proteins in eye lenses, which are responsible for the maintenance of lens transparency and proper refractive index (Wistow and Piatigorsky, 1988; De Jong et al., 1989; Wistow, 1993). The soluble S-crystallin constitutes the major lens protein in cephalopods. Morphologically, the cephalopod eyes are similar to those of the vertebrates and constitute a classical example of convergent evolution (Doolittle, 1988; Tomarev and Piatigorsky, 1996).

The primary amino acid sequence of S-crystallin shows an overall 41% identity with the digestive gland sigma-class glutathione transferase (GST) of cephalopod (Tomarev and Zinovieva, 1988; Tomarev et al., 1991; Chiou et al., 1995). On the basis of crystal structure of squid sigma-class GST (Ji et al., 1995), we have constructed a tertiary structure model for the octopus lens S-crystallin (Chuang et al., 1999). In the active site region, the electrostatic potential surface calculated from the modeled structure is quite dif-

ferent from that of the authentic digestive gland sigma-GST. The positively charged environment, which stabilizes the negatively charged Meisenheimer complex intermediate in the nucleophilic aromatic substitution reaction between GSH and 2,4-dinitrochlorobenzene, is altered in S-crystallin due to the mutation of Asn-99 in sigma-GST to Asp-101 in S-crystallin (Fig. 1). This natural mutation results in the diminished GST activity of the lens S-crystallin which, however, might increase the conformational stability of the lens protein by introducing an extra ion-pair that locks the domains I and II (Fig. 1). In other words, during evolutionary recruitment of cytosolic enzyme GST for the structural function of lens protein, some mutations have taken place to endow the recruited protein with better stability at the expense of the superfluous enzymatic activity.

To maintain clarity of the lens at high concentration of lens proteins, the crystallin molecules have to arrange in some special orientation to avoid aggregation and precipitation. We provide an explanation for the unique properties of S-crystallin as compared to sigma-GST; i.e., low GST enzymatic activity and low binding affinity with the GSH affinity column (Chuang et al., 1999). In this article we further propose a novel molecular basis of S-crystallin to account for its propensity to form a long linear polymeric structure in the lens. Our model for the S-crystallin, thus, is able to explain all the characteristic properties of S-crystal-
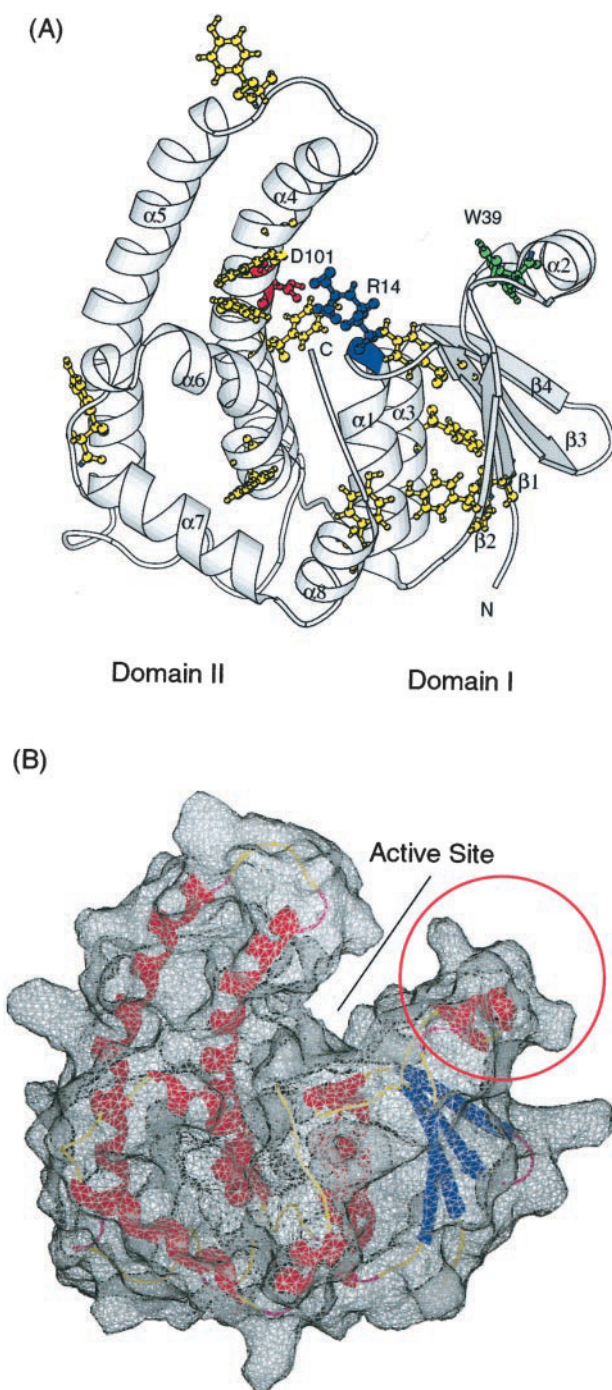
FIGURE 1 Tertiary structure of S-crystallin. (*A*) Modeled tertiary structure of octopus *S*-crystallin (Chuang et al., 1999) based on the coordinates of sigma-GST (PDB code 1gsq). The protein contains two domains. The N-terminal domain I consists of a $\beta\alpha\beta\alpha\beta\beta\alpha$ folding motif in which the $\beta$-strand is in a $\uparrow \beta2 \uparrow \beta1 \downarrow \beta3 \uparrow \beta4$ arrangement. The C-terminal domain II consists of five-stranded $\alpha$-helices in which $\alpha1$ of domain I is contacted with the lower part of $\alpha4$ in domain II. The side chain of tryptophan (*green*) (Trp-39) and tyrosine (*yellow*) residues responsible for the fluorescence of the protein are represented by ball-and-stick. The ion pair between Arg-14 (*blue*) and Asp-101 (*red*), which holds the two domains, may be responsible for the structural stability of the protein. This graph was generated by the program MOLSCRIPT (Kraulis, 1991). (*B*) Surface topology of *S*-crystallin. The backbone of the protein is colored to highlight the secondary

lin in vitro and has some implications of its optical properties in vivo.

## MATERIALS AND METHODS

### Materials

Urea and guanidinium chloride (GdmCl) were purchased from Sigma-Aldrich (St. Louis, MO). Other chemicals used were as described previously (Tang et al., 1994; Tang and Chang, 1995, 1996). *S*-Crystallin from octopus was purified to apparent homogeneity by a Sephacryl S-200 gel filtration column. The purified enzyme was subjected to sodium dodecyl sulfate-polyacrylamide gel electrophoresis (SDS/PAGE) to examine the purity (Tang et al., 1994).

### Electron microscopic analysis

A supporting membrane was made on the copper grid. One drop of *S*-crystallin solution was placed on the membrane and allowed to stand for 30 s–1 min. After the excess solution was wiped out with filter paper, one drop of phosphotungstic acid (pH 7.0) was applied and stained for 30 s–1 min. The excess solution was wiped out again. The negatively stained *S*-crystallin was examined under a transmission electron microscope (Hitachi H7000).

### Spectrofluorimetric analysis

Fluorescence spectra of the protein were monitored with a Perkin-Elmer LS-50B luminescence spectrometer at 25°C. All spectra were corrected for the buffer absorption. The Raman spectrum of water was also corrected. The excitation wavelength was set at 280 nm or at 295 nm. Both the excitation and emission slits were set at 10 nm.

### Protein denaturation

The protein was incubated with various concentrations of urea or GdmCl in Tris-HCl buffer (50 mM, pH 7.4) at 25°C for 30 min. The maximum peak of the fluorescence emission spectrum and decrease in fluorescence intensity at maximum peak were used to monitor the denaturation process. Each spectrum was corrected for the corresponding reagent blank. The Raman spectrum of water was also corrected.

### Light-scattering measurements

Polymerization and aggregation of the urea- or GdmCl-treated *S*-crystallin was measured by light scattering at 340 nm with a Perkin-Elmer Lambda-3B spectrophotometer. The protein precipitate was found to be insoluble in Tris-HCl buffer (50 mM, pH 7.4) but was soluble in high concentration of denaturant. In the pH studies, the same buffer (bis-Tris-propane-acetate) was used throughout the whole pH range to avoid the buffer or ionic strength effect.

Phase diagrams of the *S*-crystallin were constructed by combining light scattering and the cloud-point method at various protein and denaturant concentrations. The appearance of light scattering for a transparent solution

structure, $\alpha$-helices in red, $\beta$-sheets in blue, $\beta$-turn in purple, and random coil in yellow. The circle represents the region whose structural change reflected in the fluorescence changes at 358 nm. A point indicates the active site region. This structure was generated by the program SPOCK (web site: http://quorum.tamu.edu/jon/spock/).

was taken as an indication of polymerization, and the opacity of the solution was regarded as an indication of aggregation.

## RESULTS

### Molecular structure of the octopus lens *S*-crystallin

The modeled tertiary structure of *S*-crystallin has an overall topology similar to the cytosolic detoxification enzyme GST, which contains two domains per monomer (Chuang et al., 1999). The N-terminal domain I is an $\alpha/\beta$ structure, built up of four-stranded $\beta$-sheets and three $\alpha$-helices that represent a typical GSH binding domain of the $\beta\alpha\beta\alpha(\alpha)\beta\beta\alpha$ folding pattern (Gilliland, 1993). The C-terminal domain II, like other GSTs, contains five-stranded $\alpha$-helices folded in a similar pattern (Fig. 1 *A*). There is a short linker region (Gly-77–Phe-78–His-79–Gly-80–Arg-81) that links the N-terminal and C-terminal domains. There is only one tryptophanyl residue (Trp-39) in the molecule located at the $\alpha2$ helical region. The 10 tyrosyl residues are scattered around the whole molecule. These aromatic residues are responsible for the fluorescence observed for *S*-crystallin. The surface topology of the protein clearly shows an active site region between domains I and II (Fig. 1 *B*), which is occluded as compared to sigma-GST (Ji et al., 1995; Chuang et al., 1999).

The morphology of *S*-crystallin was examined by using a transmission electron microscope. Various polymeric forms including monomer, dimer, trimer, and polymer were observed for the native protein (Fig. 2). *S*-Crystallin has a high tendency of aggregation and precipitation. The aggregate, whether it is formed spontaneously upon storage or chemically induced by urea or GdmCl, does not show any regular structure (Fig. 2 *C*). This aggregate is thus envisioned as an entangled network of unfolded polypeptides. To further examine the polymerization and aggregation properties of this lens protein, we studied the fluorescence and light scattering properties of the protein in the presence of GdmCl or urea.

### Reversible denaturation of *S*-crystallin in GdmCl or urea

The intrinsic fluorescence of a protein is a sensitive probe to monitor the conformational change of that protein. When excited at 280 nm, the native *S*-crystallin showed a broad fluorescence spectrum with a maximum at 340 and a shoulder at 320 nm. After denaturing with GdmCl, two maximum emission fluorescence peaks at 358 nm and 310 nm, respectively, were clearly observed (Fig. 3 *A*). The fluorescence intensity was quenched. However, if the protein was excited at 295, which only excites the tryptophanyl chromophore, the native protein exhibited only one fluorescence peak at 338 nm, as expected, and shifted to 360 nm in the denatured
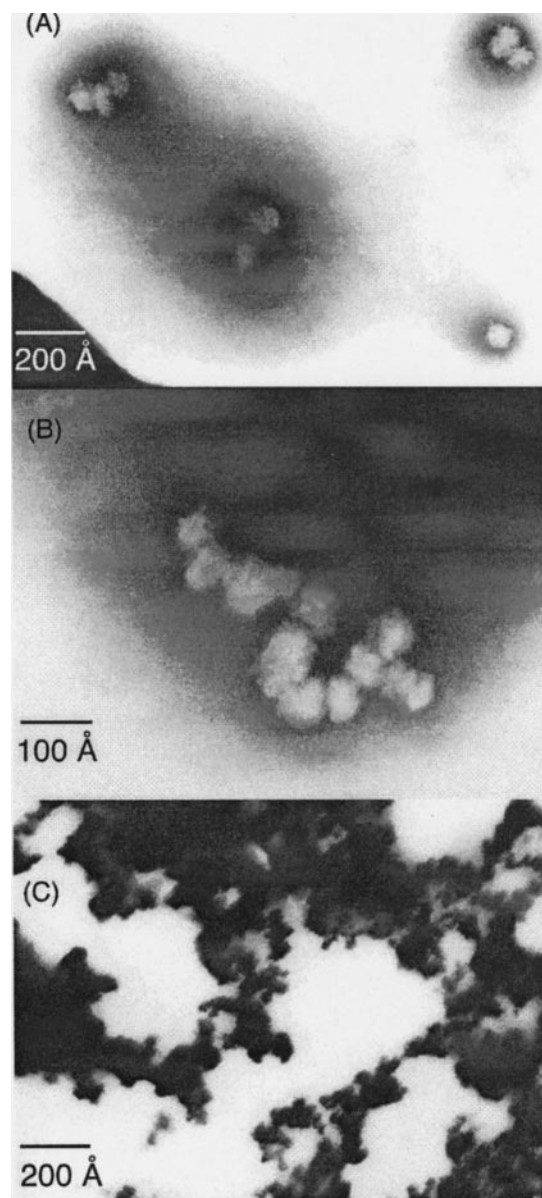


FIGURE 2 Electron micrograph of *S*-crystallin. Native *S*-crystallin in Tris-HCl buffer (50 mM, pH 7.5, containing 5 mM EDTA), negatively stained with phosphotungstic acid, was examined by electron microscope at 40,000× showing the monomer, dimer, and trimer (*A*) or 80,000× magnification showing the polymer (*B*). (*C*) The aggregate of the GdmCl (80 mM)-treated *S*-crystallin was shown at 40,000× magnification. The bars represent the dimension of the molecule.

protein. This fluorescence thus reflects the conformational changes around the $\alpha2$ helical region (circled in Fig. 1 *B*).

Urea has a similar effect on the protein intrinsic fluorescence of Trp-39 to that of GdmCl, but is found to be less effective as a denaturant to induce the gross conformational change, as indicated in Fig. 3 *B*. The denatured protein shows only shifting of the 338 nm peak with little change at 320 nm. Both the urea- and GdmCl-induced denaturation were found to be reversible (Fig. 3).
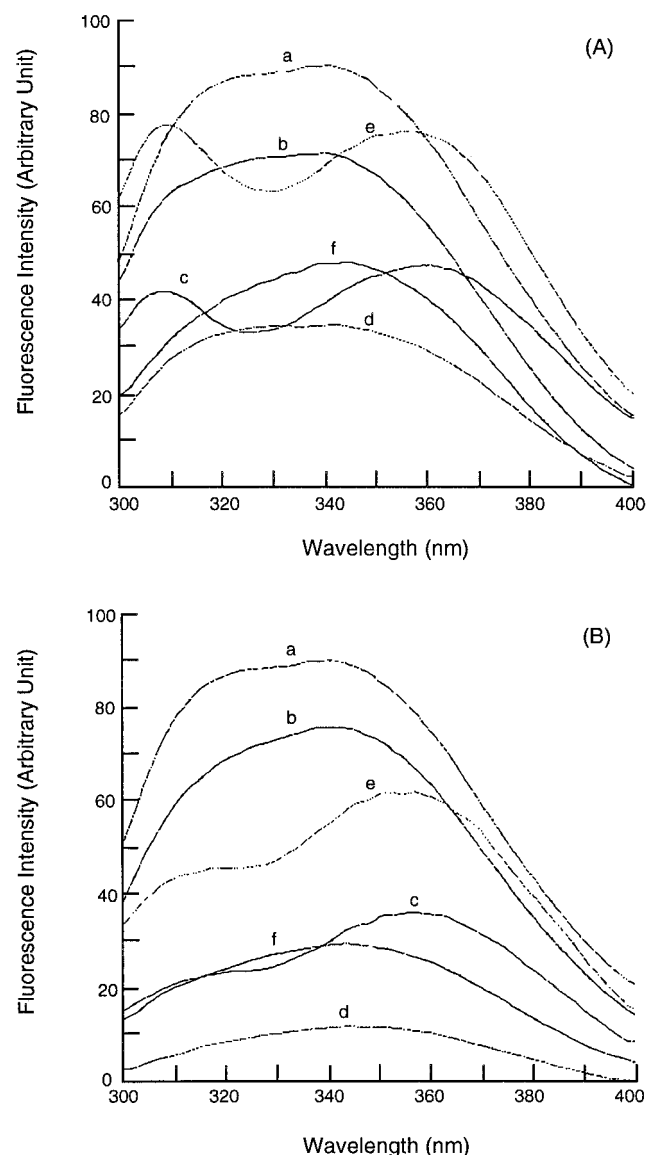
FIGURE 3 Reversible fluorescence changes of *S*-crystallin in the presence of urea or GdmCl. The protein in Tris-HCl buffer (50 mM, pH 7.5, containing 5 mM EDTA) was treated with GdmCl (*A*) or urea (*B*) for 30 min and the fluorescence emission spectrum was monitored at 280 nm excitation wavelength. In (*A*), *curve a* is the native *S*-crystallin (protein concentration 25.5 $\mu$g/ml); *curve b* is the *S*-crystallin in 0.006 M GdmCl (protein concentration 25.5 $\mu$g/ml); *curve c* is the *S*-crystallin in 3.6 M GdmCl (protein concentration 10.2 $\mu$g/ml); *curve d* is the dilution solution of *c* to final GdmCl concentration of 0.006 M (protein concentration 3.4 $\mu$g/ml); *curve e* represents the *S*-crystallin precipitated with 1.2 M GdmCl, the precipitate was collected by centrifugation and dissolved in 3.6 M GdmCl; *curve f* is the dilution of *e* to give a final GdmCl concentration of 0.006 M (final protein concentration 6.7 $\mu$g/ml). In (*B*), *curve a* is the native *S*-crystallin at 25.5 $\mu$g/ml; *curve b* is the *S*-crystallin in 0.024 M urea (protein concentration 25.5 $\mu$g/ml); *curve c* is the *S*-crystallin in 8.1 M urea (protein concentration 50.1 $\mu$g/ml); *curve d* is the dilution solution of *c* to final urea concentration of 0.024 M (protein concentration 15.3 $\mu$g/ml); *curve e* represents the *S*-crystallin precipitated with 3.15 M urea, the precipitate was collected by centrifugation and dissolved in 8.1 M urea; *curve f* is the dilution of *e* to give a final urea concentration of 0.024 M (final protein concentration 4.73 $\mu$g/ml).

## Quaternary structural changes of *S*-crystallin in GdmCl or urea

In the intermediate denaturant concentrations the protein polymerized and finally aggregated, as manifested by light scattering and precipitation. The appearance of light scattering has a delay time ($t_d$) (Fig. 4 *A*), which is dependent on protein concentration (Fig. 4 *B*) and may suggest a nucleation mechanism for the polymer formation. However, a log-log plot of the *S*-crystallin concentration dependence of
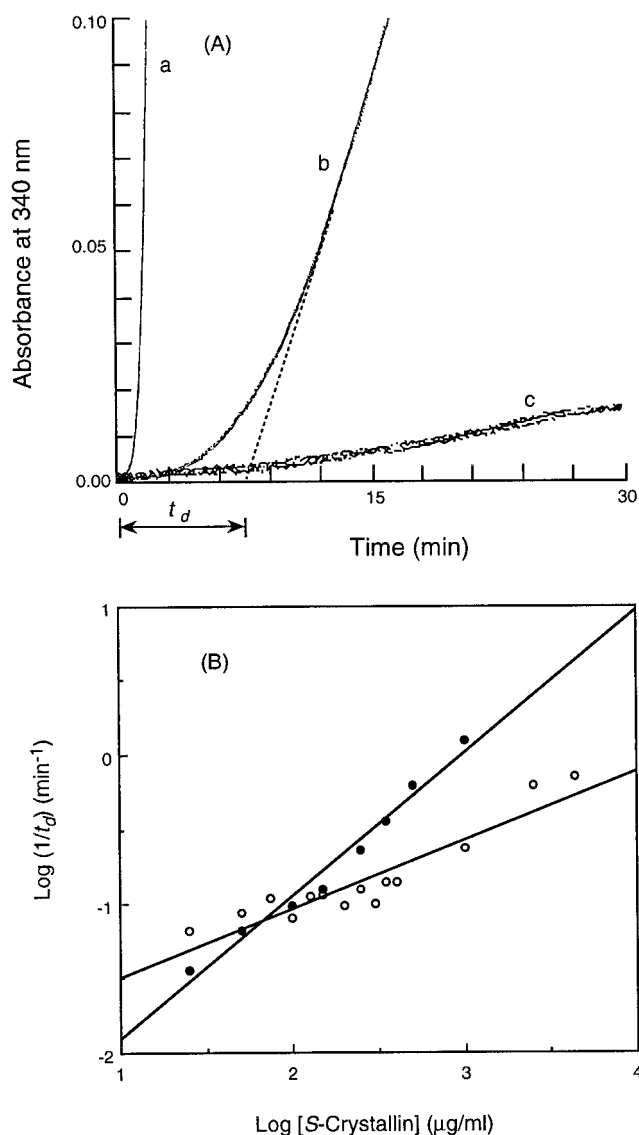


FIGURE 4 Denaturant-induced light scattering of *S*-crystallin. (*A*) Recorder tracing of the light scattering of *S*-crystallin in Tris-HCl buffer (50 mM, pH 7.5, containing 5 mM EDTA) in the presence of 3.52 M urea. Extrapolating the steady-state region (*dashed line*) to the horizontal axis gave the delay time ($t_d$) for the onset of light scattering. The *S*-crystallin concentration was (*a*) 350, (*b*) 150, and (*c*) 50 $\mu$g/ml, respectively. (*B*) The delay time ($t_d$) in *S*-crystallin polymerization was plotted versus *S*-crystallin concentration in double logarithmic plot at two urea concentrations: (●) 3.52 M, (○) 1.1 M, respectively. GdmCl gave similar results.

$1/t_d$ gave slopes approaching unity, which essentially rules out the nucleation mechanism (Hofrichter et al., 1974). The slope of the steady-state region (*dashed line* in Fig. 4 *A*, *curve b*) was taken as the steady-state polymerization rate in other experiments.

When the light scattering of the protein solution was examined at various concentrations of denaturant, the data were bell-shaped and reached a maximum at certain denaturant concentration, which was also found to be dependent on protein concentration (Fig. 5, *A* and *B*). Phase diagrams for the quaternary structural change of *S*-crystallin in urea and GdmCl solution were constructed (Fig. 5, *C* and *D*). GdmCl-induced polymerization and aggregation is in a nar-

rower range than urea-induced polymerization and aggregation. At sufficient diluted protein concentration (~30 µg/ml), neither urea nor GdmCl can induce precipitation of *S*-crystallin. Theoretically, at infinite dilution of protein solution no polymer can be formed and *S*-crystallin is in equilibrium between the folded state and the unfolded state at ~2 M urea or 0.9 M GdmCl concentration.

## Effect of salt on the polymerization of octopus *S*-crystallin

The possible interactions for the polymerization of *S*-crystallin were accessed by examining the effects of salt, pH,
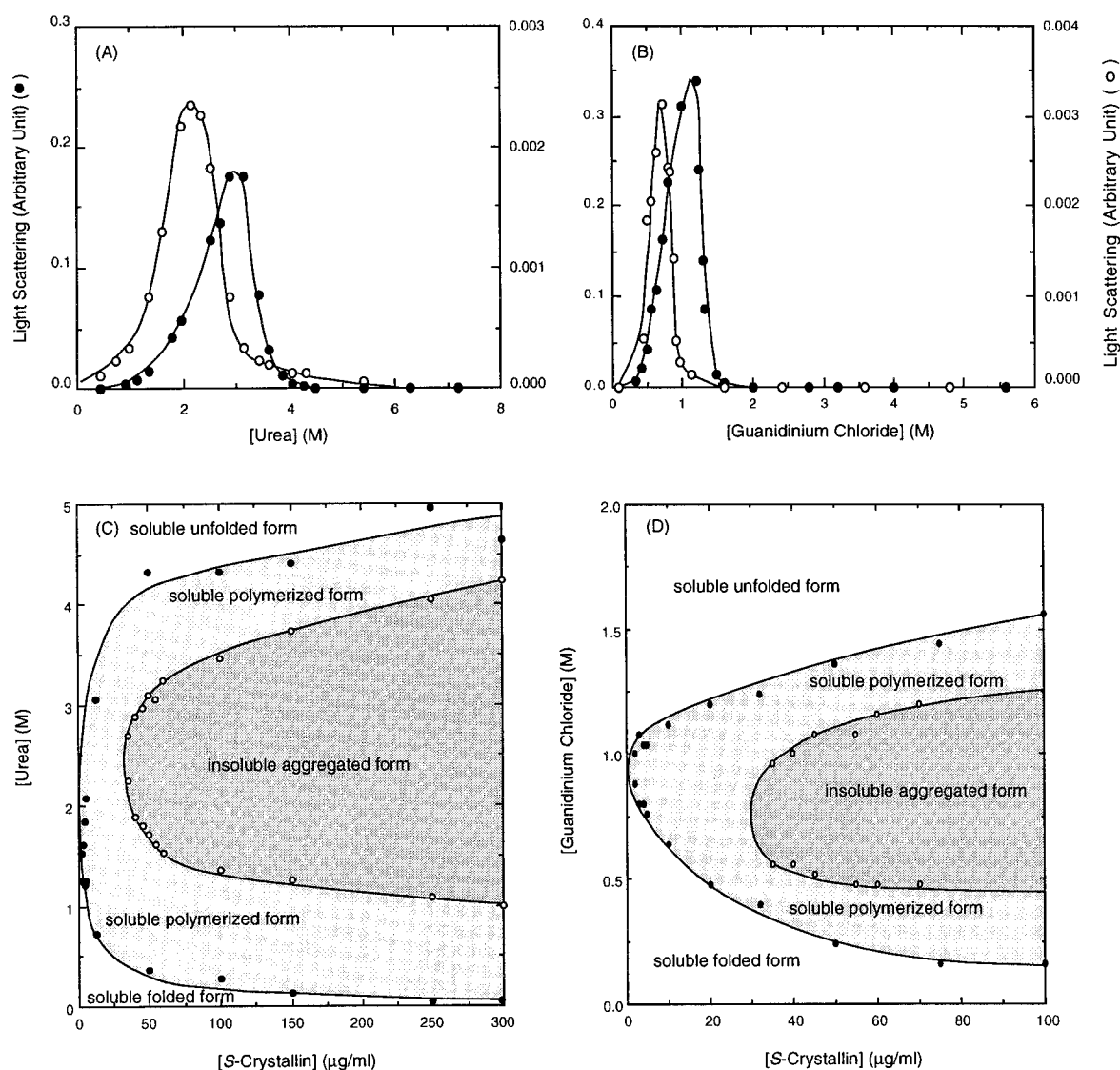


FIGURE 5   Phase diagrams for *S*-crystallin in urea or GdmCl solution. (*A* and *B*) Light scattering of *S*-crystallin as measured by the steady-state slopes of the recorder tracing, as shown in Fig. 4 *A*, was plotted versus denaturant concentration at two protein concentrations (○) 23.5 µg/ml, (●) 238.2 µg/ml. (*C* and *D*) The light scattering detected by spectrophotometer and the visually observed opacity were used to construct the phase diagram of *S*-crystallin. The upper white area denotes the soluble unfolded denatured form, while the lower white area denotes the soluble monomeric or oligomeric form. The gray area shows the soluble polymeric form, detected by light scattering. The dark area represents the insoluble aggregated form observed by the opacity of the solution.

and temperature on the rates of polymerization. Since GdmCl is more efficient than urea in inducing the polymerization and aggregation of *S*-crystallin, we checked the light scattering of *S*-crystallin polymerization delay time in urea in the presence of NaCl. With increasing NaCl concentration, the slope of the double logarithmic plot of $1/t_d$ versus *S*-crystallin concentration increased (Fig. 6). The efficiency of GdmCl thus, at least in part, is due to the ionic strength effect.

## Effect of pH and temperature on the polymerization of octopus *S*-crystallin

The polymerization of *S*-crystallin was also examined at various pH values of the solution. The native protein shows complex pH dependency of the polymerization rate indicating involvement of multiple ionic interactions in the process. Both urea and GdmCl show similar pH effect on the pH dependency of the polymerization rate, but are different from the native protein in the basic region (Fig. 7).

Under similar conditions as those described in Fig. 7, the protein started to polymerize at 30°C. The polymerization rate increased at high temperature (Fig. 8 *A*) and finally induced aggregation. The aggregate did not dissolve in buffer solution and was redissolved in high concentration of denaturant. An Arrhenius plot of the natural logarithm of the steady-state polymerization rate versus reciprocal of absolute temperature was biphasic (Fig. 8 *B*). At protein concentration of 26 $\mu$g/ml, the inflection point was at 45°C. The activation energies were 21.9 kcal/mol and 11.4 kcal/mol, respectively, for the two segments. When the protein concentration was elevated to 260 $\mu$g/ml, the inflection point

lowered to 40°C with activation energies of 36.2 kcal/mol and 8.3 kcal/mol. These two segments were presumably attributed to the formation of soluble polymers and insoluble aggregates, respectively. The temperature dependence of polymerization of *S*-crystallin indicates the involvement of hydrophobic interactions between protomers as well.

## Surface analysis of the *S*-crystallin molecule

The surface properties of the molecule were analyzed with the SPOCK program. No obvious difference is observed in the surface hydrophobicity between *S*-crystallin and sigma-GST. However, as shown in Fig. 9, the surface charge distribution is quite different between these two proteins. In one side of the *S*-crystallin molecule there is a negatively charged region (the small circle in Fig. 9 *A*) surrounded by positively charged residues (the blue region circled between the large and the small circles). The corresponding residues responsible for this region are Arg-14/Arg-13, Arg-70/Arg-69, Arg-105/Lys-104, His-108/Phe-107, Arg-128/Val-116, Arg-129/Gln-117, Arg-131/Asn-119, Arg-137/Lys-125, Arg-138/Arg-126 in *S*-crystallin and sigma-GST, respectively. Four of these residues are not charged in sigma-GST, which makes the corresponding area in sigma-GST less obvious in positive charge (less intense blue color in Fig. 9 *D*) except at the active site region. When the *S*-crystallin molecule is rotated clockwise around the *y* axis by 180°, the opposite side of the molecule shows a clear contrast charge distribution (Fig. 9 *B*). Now the small circle encloses a positively charged blue region, which is surrounded by
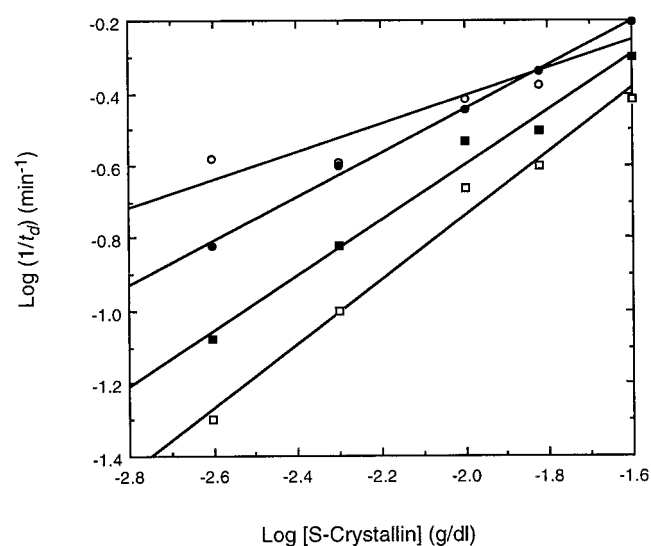


FIGURE 6   Effect of salt on the polymerization rate of *S*-crystallin in urea. The delay time of *S*-crystallin polymerization in Tris-HCl buffer (50 mM, pH 7.5, containing 5 mM EDTA) in the presence of various amounts of salt was plotted versus *S*-crystallin concentrations in double logarithmic plot. From top to bottom, the NaCl concentration was 0 M (○), 0.5 M (●), 2.0 M (■), and 3.6 M (□), respectively.
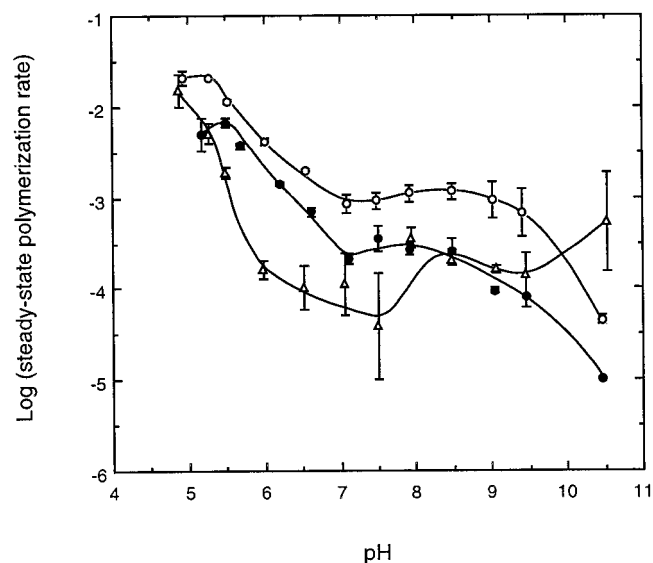
FIGURE 7   Effect of pH on the polymerization rate of *S*-crystallin in urea or GdmCl. The steady-state polymerization rates of *S*-crystallin (25.4 $\mu$g/ml in 230 mM bis-Tris-propane-acetate buffer) at different pH values were recorded in the presence of 0.72 M GdmCl (○), or 2.16 M urea (●), or without any denaturant added (△). Error bars represent the mean standard errors.
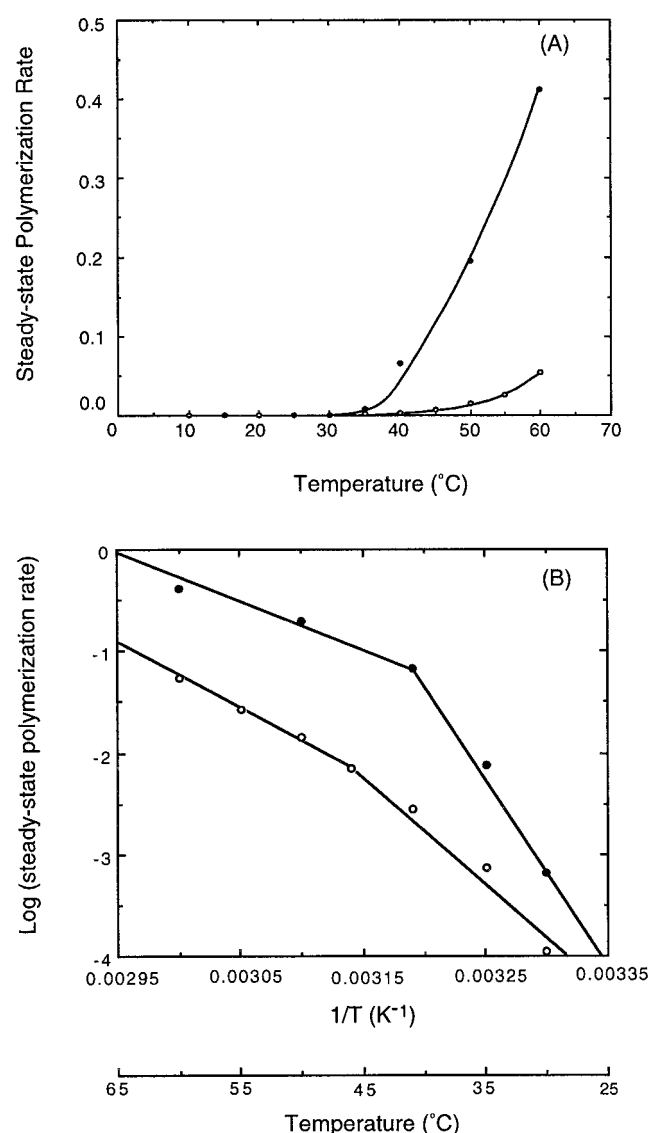
FIGURE 8  Effect of temperature on the polymerization rate of S-crystallin. (A) The steady-state polymerization rates of S-crystallin (○, 26 μg/ml; ●, 260 μg/ml) in Tris-HCl buffer (50 mM, pH 7.5, containing 5 mM EDTA) at different temperatures were recorded. (B) Arrhenius plots of the data shown in (A).

clusters of negatively charged red region. This complementary charge distribution in the opposite side of the molecule is much less obvious in sigma-GST (Fig. 9, D and E).

The structure complementation in the opposite side of S-crystallin is more clearly shown when the molecule is rotated clockwise around the y axis by 90° (Fig. 9 C). In one side (left) of the molecule, there is a protrusion from the side chain of Lys-208 (point a) and is shown in blue. On the opposite side (right) of the molecule, there is a cleft in the red color (point b) contributed by seven aspartate residues (Asp-90, Asp-94, Asp-98, Asp-101, Asp-102, Asp-179, and Asp-180), in which three of them (residues 101, 179, and 180) are Asn, His, and Thr, respectively, in sigma-GST. The

side chain of Lys-208 can be fitted perfectly into the negatively charged cleft of another protomer.

## DISCUSSION

Lens is a specialized tissue. In vertebrates, the lens epithelial cell loses its nucleus and other cell organelles during growth. Therefore, there is no metabolism of the lens proteins (Wistow and Piatigorsky, 1988; De Jong et al., 1989). For this reason lens proteins must be reasonably stable and be able to resist oxidative stress during the life span. The imaging system of cephalopods has some similarities to those of the vertebrates (Doolittle, 1988; Tomarev and Piatigorsky, 1996). However, the purified octopus lens protein, S-crystallin, is easily aggregated in vitro, which will cause a cataract if it occurs in vivo. When examined by electron microscope, various polymerized forms of S-crystallin were observed (Fig. 2). Since these quaternary structures of S-crystallin were observed in vitro on diluted protein concentration, it is an intriguing question to determine the quaternary structure of S-crystallin in vivo. It is thus important to characterize the factors that affect the polymerization and aggregation of the protein. We used urea and GdmCl as denaturant and utilized the intrinsic fluorescence of S-crystallin as the structural probe to examine the conformational stability of the protein.

At high concentration of GdmCl, two fluorescence peaks are observed. Since S-crystallin contains only one tryptophan (Trp-39 in the α2 helix), the fluorescence peak at 358 nm thus reports the conformational change in the area shown in Fig. 1 B by a circle. This lobe constitutes the GSH binding site of the molecule, and Trp-39 is proposed to be directly involved in GSH binding (Ji et al., 1995). The fluorescence at 358 nm thus suggests a localized conformational change of the GSH binding site. The fluorescence peak at 320 nm, however, reflects the gross conformational change of the whole molecule, as the protein contains 10 tyrosine residues (Tyr-4, Tyr-8, Tyr-29, Tyr-69, Tyr-97, Tyr-103, Tyr-107, Tyr-120, Tyr-170, and Tyr-206), which are scattered around both N-terminal and C-terminal domains (Fig. 1 A). The clear separation of these two fluorescence peaks indicates no energy transfer of tyrosine fluorescence by tryptophan. This is in accordance with the structure shown in Fig. 1, which indicates that Trp-39 is located in the isolated α2 helix. There is no direct contact between Trp-39 and any tyrosine residue. The presence of two glycine residues at the hinge region might imply that the linker region has some structural flexibility. However, the extra ion-pair between Asp-101 and Arg-14 introduced by the Asn to Asp mutation in S-crystallin suggests that domains I and II should be held more tightly than in sigma-GST.

When the protein was treated with intermediate concentrations of chemical denaturant, polymerization and aggregation occurred. However, when examined under an electron microscope the aggregate shows irregular structure, and no tubule structure was observed (Fig. 2 C). The ag-
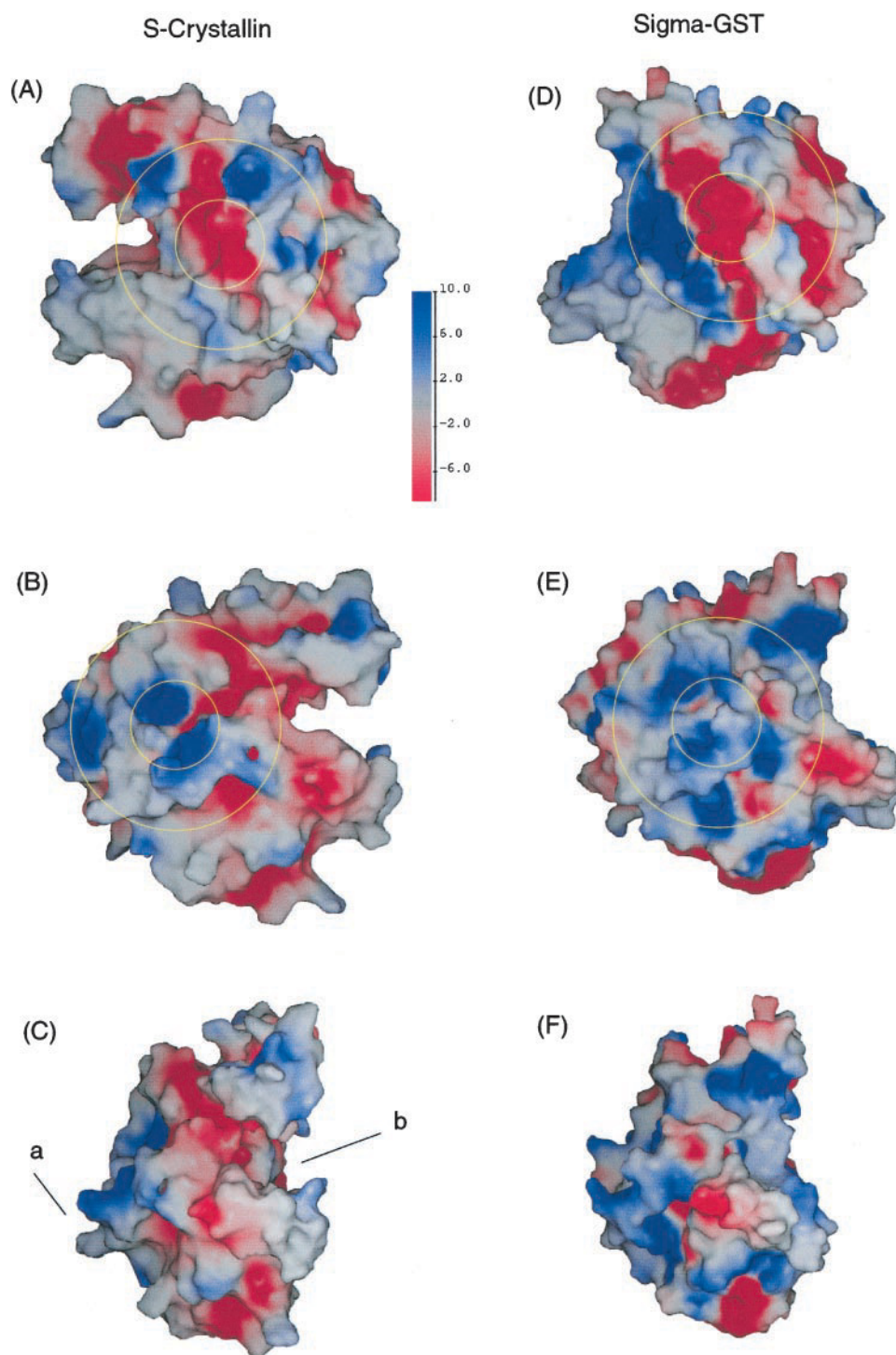
FIGURE 9 Comparison of the surface electric potential of *S*-crystallin and sigma-GST monomers. Both *S*-crystallin (*A–C*) and sigma-GST (*D–F*) are in the same orientation where *B* and *E* are the opposite side of *A* and *D*, respectively. Areas of positive potential are shown in blue and those with negative potential are in red. The salient electrostatic differences between *S*-crystallin and sigma-GST in the opposite sides are shown in the area highlighted with circles. (*A*) and (*B*) are *S*-crystallin molecules rotated clockwise along the *y* axis by 180°, showing the opposite surface of the molecule. The two circles on each side show the distinguish charge distribution areas. In (*A*), the small circle enclosed a deep red color region, which is surrounded by blue area. On the other site (*B*), the charge distribution is opposite in the two circles. The small circle enclosed a blue region, which is surrounded by red area. These charge complementation is less prominent in sigma-GST (*D* and *E*). The surface complementation of *S*-crystallin is more clear when the molecules of *S*-crystallin and sigma-GST shown in *A* and *D* were rotated clockwise along the *y* axis to 90°, which produces a view from top of the active site region. The geometric complementation fit of the two opposite sides of *S*-crystallin is prominent (*C*). The left side is convex, whereas the right side is concave. Furthermore, as indicated by point *a*, the protruded Lys-208 is positively charged, and a cluster of aspartate residues constitutes the negatively charged

gregate therefore should be from the partially unfolded form (possibly a molten globule state) of the protein, which has the tendency to precipitate (Ptitsyn, 1995; Jaenicke, 1996; Kuwajima, 1996; Dill, 1999; Tsai et al., 1999). Because the linear polymer of the native protein was observed, we propose that in the lens, $S$-crystallin, at high concentration, exists as an irregular linear polymer ($P_n$, Fig. 10), which dissociates under low protein concentration during the extraction procedure to lower polymerized states ($P_1 \cdots P_{n-1}$). In the presence of denaturant, the protein unfolded to a form, $P_x$, which is prone to form insoluble aggregate (A) in vitro. Dissolving this aggregate in a high concentration of denaturant completely unfolded the protein (U). High pressure (200–300 m below sea level), low temperature (4°C), and high protein concentration, where the octopus lens exists in the deep sea, might be the critical factors for $S$-crystallin to maintain a soluble polymerized form and keep the lens transparent (Siezen and Shaw, 1982).

To explain the results described in this article, we propose a molecular model of $S$-crystallin that might exist in vivo. A reliable molecular model for $S$-crystallin must be able to explain the following three properties that are characteristics for $S$-crystallin versus the authentic sigma-GST: 1) the octopus $S$-crystallin is not bound to the GSH column (Tang et al., 1994). Most GSTs, however, have high affinity with GSH. In many cases, a single GSH-Sepharose affinity column is enough to purify the enzyme from the crude cell extract to apparently homogeneity. We have successfully purified the octopus digestive gland sigma-GST to apparent homogeneity by this single affinity column step. However, the same procedure did not work for $S$-crystallin (Tang et al., 1994). 2) $S$-Crystallin possesses very little endogenous GST activity in the nucleophilic aromatic substitution reaction ($S_NAr$) between GSH and 2,4-dinitrochlorobenzene. Octopus S-crystallin possesses only ~1/2000 $S_NAr$ activity as compared to the digestive gland sigma-GST (Tang et al., 1994). 3) $S$-Crystallin can be more easily aggregated in solution than sigma-GST. After extraction from the lens, $S$-crystallin cannot tolerate a freezing and thawing process, even upon storage at 4°C in the neutral buffer solution; $S$-crystallin precipitates in a few days, while a sigma-GST solution can be frozen for a couple of months.

The molecular model proposed previously provides an explicit explanation for the first two propensities of $S$-crystallin (Chuang et al., 1999). In the active site region, the electrostatic potential surface calculated from the modeled $S$-crystallin structure is quite different from that of squid sigma-GST. The positively charged environment, which contributes to stabilizing the negatively charged Meisenheimer complex intermediate, is altered in $S$-crystallin due to the mutation of Asn-99 in sigma-GST to Asp-101 in $S$-crystallin. Furthermore, the important Phe-106 in Sigma-GST is changed to His-108 in $S$-crystallin. These differ-
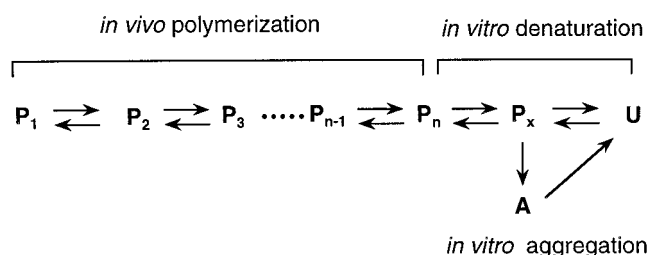


FIGURE 10 Proposed quaternary structural changes of $S$-crystallin in vivo and in vitro. $P_1$ to $P_n$ represent the various soluble polymer units of $S$-crystallin found in the lens. $P_x$ denotes a partially unfolded state (possibly a molten globule state), which is prone to aggregate. U and A represent the soluble unfolded and insoluble aggregated forms, respectively.

ences might change the substrate specificities of $S$-crystallin to adapt the oxidative and high-pressure environment in the deep sea where the cephalopods live. The $S$-crystallin structure has longer $\alpha 4$ and $\alpha 5$ chains, corresponding to an 11-amino acid residue insertion between the conserved $\alpha 4$ and $\alpha 5$ segments. This insertion makes the active center region of $S$-crystallin in a more closed conformation than the sigma-class GST (Fig. 1 $B$). However, a previously proposed molecular structure of $S$-crystallin (Chuang et al., 1999) does not provide an explanation for the aggregation propensity of $S$-crystallin.

Here we propose the molecular basis for the $S$-crystallin polymerization in lenses as suggested by the surface analysis of the lens protein. We propose that, due to the charge and structural complementary association between protomers by a side-by-side manner, $S$-crystallin can form an endless polymer, as shown in Fig. 11. The polymer could be started from a monomeric (Fig. 11 $A$) or, more likely, from a dimeric structure with the addition of either monomers (Fig. 11 $B$) or dimers (Fig. 11 $C$) on both sides of a dimer. The interfacial region between monomers in a dimer involves $\alpha 3$-$\alpha 5$ and $\beta 4$ elements, and does not shield the structure complement regions proposed in this study. However, sigma-GST lacks this structural complementation (Fig. 9 $F$) and is less likely to polymerize. Our present model can use the same arguments to explain the low endogenous $S_NAr$ activity of GST and the low binding affinity of $S$-crystallin to the GSH affinity column, as described previously (Chuang et al., 1999). This model presents a further explanation for the polymerization propensity of $S$-crystallin and is compatible with the recent finding that lens crystallins, in a highly concentrated solution, are structurally rather compact (Liang and Chakrabarti, 1998). Close packing of $S$-crystallin, such as the model shown in Fig. 11, which lacks of a regular underlying lattice organization but can lead to a short-range, liquid-like structure order, may account for the transparency of the lens. This

center (point $b$). This negatively charged center further forms a cleft that fits the Lys-208 from another protomer perfectly. This structural complementation is not observed in sigma-GST ($F$). These figures were generated by the program SPOCK (web site: http://quorum.tamu.edu/jon/spock/).
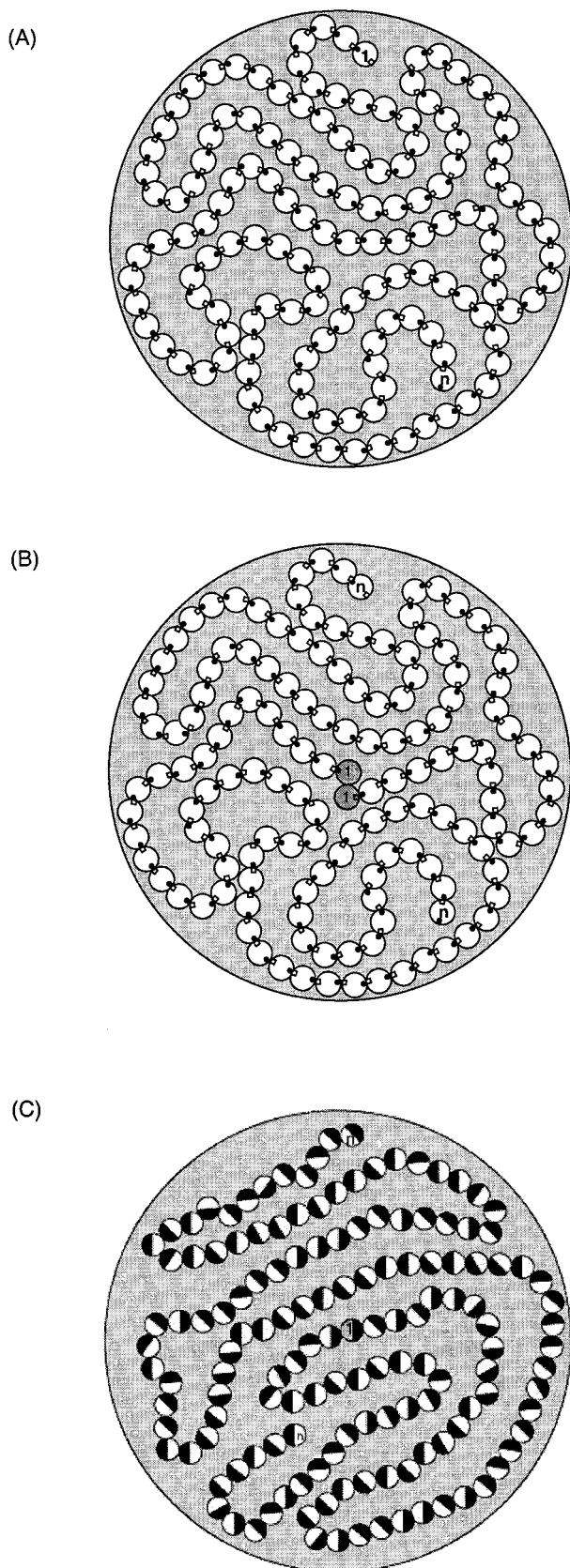
glass-like short-range order structure has been demonstrated experimentally for α-crystallin (Delaye and Tardieu, 1983, Vérétout et al., 1989).

Polymerization of crystallins is a major concern of these lens proteins. If aggregation occurs in vivo, it will cause opacity and cataract of the lens. It has been proposed that *S*-crystallin in cephalopods, through convergent evolution, has developed a structure that resembles the β-crystallin of vertebrates (Siezen and Shaw, 1982); α- and β-crystallins of vertebrates are well known to form polymers easily (Bax et al., 1990; Bennett et al., 1994, 1995). Both β- and γ-crystallins fold into two similar β-sheet domains. The main difference between these two related vertebrate eye lens proteins is the state of oligomerization. Intermolecular domain interactions result in oligomeric β-crystallin, while intramolecular contacts result in monomeric γ-crystallin (Ajaz et al., 1997). αB- and βB2-crystallins have been demonstrated to have a variable quaternary structure consisting of polydisperse size of the assembly and the subunit exchange between multimers (Haley et al., 1998; Wieligmann et al., 1998). γ-Crystallin is known to be induced by temperature of binary-liquid phase separation (Broide et al., 1991). From the x-ray crystallographic analysis, The duck delta-crystallin has also been proposed to have a linear suprahelical polymerized structure (Simpson et al., 1995). The ability to form a linear polymer may be a general phenomenon for all crystallins, and polymerization may be a general mechanism for stabilizing proteins (Slingsby, 1985; Wieligmann et al., 1998; Haley et al., 1998).

Human pi-GST was recently demonstrated to possess a temperature adaptation for the homotropic regulation of substrate binding (Caccuri et al., 1999). The temperature-induced structural changes of α-crystallin are crucial for its chaperone-like activity (Raman and Rao, 1997). Although briefly mentioned previously (Tomarev and Piatigorsky, 1996), the possibility of *S*-crystallin possessing a chaperone-like activity has not yet been demonstrated. The data shown in Fig. 8 indicate a temperature-dependent structural change of *S*-crystallin, which might have some implications for its recruitment as the lens protein. This protein has a potential temperature modulatory ability. It is possible that, during evolution, a stable monomer is formed followed by mutation of its surface residues and result in the formation of functional polymers (Xu et al., 1998). Alternatively, a domain swapping between domain I from one protomer and

FIGURE 11  Proposed polymerized form of *S*-crystallin in octopus lens. On the basis of the molecular model as shown in Fig. 9, *S*-crystallin at high concentration in the lens is proposed to exist as a linear polymer with irregular arrangement in space. (*A*) In each protomer, the small open square and closed circle indicate the possible ionic interactions between the two circled areas as shown in Fig. 9 *C* from separate protomers. Models *B* and *C* show starting of polymer from a dimeric structure with addition of monomers (*B*) or dimers (*C*) from both sides. The gray circles in models *B* and *C* show the starting dimers. After isolation from the lens, this long-chain polymer fragmented into small polymers, as observed in electron microscopy (Fig. 2, *A* and *B*).

domain II from another protomer could also give a stable polymeric structure like that shown in Fig. 11 *A* (Bennett et al., 1994, 1995; Saint-Jean et al., 1998). However, this model seems unlikely because it proposes interactions between different domains on separate monomers, which will require disruption of not only the dimeric structure but also the domains I and II of a monomer.

## REFERENCES

Ajaz, M. S., Z. Ma, D. L. Smith, and J. B. Smith. 1997. Size of human lens β-crystallin aggregates are distinguished by N-terminal truncation of βBI. *J. Biol. Chem.* 272:11250–11255.

Bax, B., R. Lapatto, V. Nalini, H. Driessen, P. F. Lindley, D. Mahadevan, T. L. Blundell, and C. Slingsby. 1990. X-ray analysis of βB2-crystallin and evolution of oligomeric lens proteins. *Nature.* 347:776–780.

Bennett, M. J., S. Choe, and D. Eisenberg. 1994. Domain swapping: entangling alliances between proteins. *Proc. Natl. Acad. Sci. USA.* 91:3127–3131.

Bennett, M. J., M. P. Schlunegger, and D. Eisenberg. 1995. 3D domain swapping: a mechanism for oligomer assembly. *Protein Sci.* 4:2455–2468.

Broide, M. L., C. R. Berland, J. Pande, O. O. Ogun, and G. B. Benedek. 1991. Binary-liquid phase separation of lens protein solutions. *Proc. Natl. Acad. Sci. USA.* 88:5660–5664.

Caccuri, A. M., G. Antonini, P. Ascenzi, M. Nicotra, M. Nuccetelli, A. P. Mazzetti, G. Federici, M. L. Bello, and G. Ricci. 1999. Temperature adaptation of glutathione S-transferase P1-1. A case for homotropic regulation of substrate binding. *J. Biol. Chem.* 274:19276–19280.

Chiou, S. H., C. W. Yu, C. W. Lin, F. M. Pan, S. F. Lu, H. J. Lee, and G. G. Chang. 1995. Octopus *S*-crystallins with endogenous glutathione *S*-transferase (GST) activity. sequence comparison and evolutionary relationship with authentic GST enzymes. *Biochem. J.* 309:793–800.

Chuang, C. C., S. H. Wu, S. H. Chiou, and G. G. Chang. 1999. Homology modeling of cephalopod lens *S*-crystallin: a natural mutant of sigma-class glutathione transferase with diminished endogenous activity. *Biophys. J.* 76:679–690.

De Jong, W. W., W. Hendriks, J. W. M. Mulders, and H. Bloemendal. 1989. Evolution of eye lens crystallins: the stress connection. *Trends Biochem. Sci.* 14:365–368.

Delaye, M., and A. Tardieu. 1983. Short-range order of crystallin proteins accounts for eye lens transparency. *Nature.* 302:415–417.

Dill, K. A. 1999. Polymer principles and protein folding. *Protein Sci.* 8:1166–1180.

Doolittle, R. F. 1988. More molecular opportunism. *Nature.* 336:18.

Gilliland, G. L. 1993. Glutathione proteins. *Curr. Opinion Struct. Biol.* 3:875–884.

Haley, D. A., J. Horwitz, and P. L. Stewart. 1998. The small heat-shock protein, alphaB-crystallin, has a variable quaternary structure. *J. Mol. Biol.* 277:27–35.

Hofrichter, J., P. D. Ross, and W. A. Eaton. 1974. Kinetics and mechanism of deoxyhemoglobin S gelation: a new approach to understanding sickle cell disease. *Proc. Natl. Acad. Sci. USA.* 71:4865–4867.

Jaenicke, R. 1996. Protein folding and association: in vitro studies for self-organization and targeting in the cell. *Curr. Top. Cell. Regul.* 34:209–314.

Ji, X., E. C. von Rosenvinge, W. W. Johnson, S. I. Tomarev, J. Piatigorsky, R. N. Armstrong, and G. L. Gilliland. 1995. Three-dimensional structure, catalytic properties, and evolution of a sigma class glutathione transferase from squid, a progenitor of the lens *S*-crystallins of cephalopods. *Biochemistry.* 34:5317–5328.

Kraulis, P. 1991. MOLSCRIPT: a program to produce both detailed and schematic plots of protein structures. *J. Appl. Crystallogr.* 24:946–950.

Kuwajima, K. 1996. The molten globule state of α-lactalbumin. *FASEB J.* 10:102–109.

Liang, J. J-N., and B. Chakrabarti. 1998. Intermolecular interactions of lens proteins: from rotational mobile to immobile states at high protein concentrations. *Biochem. Biophys. Res. Commun.* 246:441–445.

Ptitsyn, O. B. 1995. Molten globule and protein folding. *Adv. Protein Chem.* 47:83–229.

Raman, B., and Ch. M. Rao. 1997. Chaperone-like activity and temperature-induced structural changes of α-crystallin. *J. Biol. Chem.* 272:23559–23564.

Saint-Jean, A. P., K. R. Phillips, D. J. Creighton, and M. J. Stone. 1998. Active monomeric and dimeric forms of *Pseudomonas putida* glyoxalase I: evidence for 3D domain swapping. *Biochemistry.* 37:10345–10353.

Siezen, R. J., and D. C. Shaw. 1982. Physicochemical characterization of lens proteins of the squid *Nototodarus gouldi* and comparison with vertebrate crystallins. *Biochim. Biophys. Acta.* 704:304–320.

Simpson, A., D. Moss, and C. Slingsby. 1995. The avian eye lens protein δ-crystallin shows a novel packing arrangement of tetramers in a supramolecular helix. *Structure.* 3:403–412.

Slingsby, C. 1985. Structural variation in lens crystallins. *Trends Biochem. Sci.* 10:281–284.

Tang, S. S., and G. G. Chang. 1995. Steady-state kinetics and chemical mechanism of octopus hepatopancreatic glutathione transferase. *Biochem. J.* 309:347–353.

Tang, S. S., and G. G. Chang. 1996. Kinetic characterization of the endogenous glutathione transferase activity of octopus lens *S*-crystallin. *J. Biochem.* 119:1182–1188.

Tang, S. S., C. C. Lin, and G. G. Chang. 1994. Isolation and characterization of octopus hepatopancreatic glutathione *S*-transferase. Comparison of digestive gland enzyme with lens *S*-crystallin. *J. Protein Chem.* 13:609–618.

Tomarev, S. I., and J. Piatigorsky. 1996. Lens crystallins of invertebrates. Diversity and recruitment from detoxification enzymes and novel proteins. *Eur. J. Biochem.* 235:449–465.

Tomarev, S. I., and R. D. Zinovieva. 1988. Squid major lens polypeptides are homologous to glutathione S-transferase subunits. *Nature.* 336:86–88.

Tomarev, S. I., R. D. Zinovieva, and J. Piatigorsky. 1991. Crystallins of the octopus lens. Recruitment from detoxification enzymes. *J. Biol. Chem.* 266:24226–24231.

Tsai, C. J., S. Kumar, B. Ma, and R. Nussinov. 1999. Folding funnels, binding funnels, and protein function. *Protein Sci.* 8:1181–1190.

Vérétout, F., M. Delaye, and A. Tardieu. 1989. Molecular basis of eye lens transparency. osmotic pressure and x-ray analysis of α-crystallin solutions. *J. Mol. Biol.* 205:713–728.

Wieligmann, K., B. Norledge, R. Jaenicke, and E.-M. Mayr. 1998. Eye lens betaB2-crystallin: circular permutation does not influence the oligomerization state but enhances the conformational stability. *J. Mol. Biol.* 280:721–729.

Wistow, G. J. 1993. Lens crystallins: gene recruitment and evolutionary dynamism. *Trends Biochem. Sci* 18:301–306.

Wistow, G. J., and J. Piatigorsky. 1988. Lens crystallins: the evolution and expression of proteins for a highly specialized tissue. *Annu. Rev. Biochem.* 57:479–504.

Xu, D., C. J. Tsai, and R. Nussinov. 1998. Mechanism and evolution of protein dimerization. *Protein Sci.* 7:533–544.